SOFTWARE FOCUS



libwfa: Wavefunction analysis tools for excited and open-shell electronic states

Felix Plasser¹

| Anna I. Krylov² | Andreas Dreuw³

¹Department of Chemistry, Loughborough University, Loughborough, UK

²Department of Chemistry, University of Southern California, California, Los Angeles, USA

³Interdisciplinary Center for Scientific Computing, Ruprecht-Karls University, Heidelberg, Germany

Correspondence

Felix Plasser, Department of Chemistry, Loughborough University, Loughborough, LE11 3TU, UK.

Email: f.plasser@lboro.ac.uk

Funding information

National Science Foundation, Grant/ Award Number: CHE-1856342; U.S. Department of Energy, Grant/Award Number: DE-SC0018910

Edited by: Peter R. Schreiner, Editor-in-Chief

Abstract

An open-source software library for wavefunction analysis, libwfa, provides a comprehensive and flexible toolbox for post-processing excited-state calculations, featuring a hierarchy of interconnected visual and quantitative analysis methods. These tools afford compact graphical representations of various excited-state processes, provide detailed insight into electronic structure, and are suitable for automated processing of large data sets. The analysis is based on reduced quantities, such as state and transition density matrices (DMs), and allows one to distill simple molecular orbital pictures of physical phenomena from intricate correlated wavefunctions. The implemented descriptors provide a rigorous link between many-body wavefunctions and intuitive physical and chemical models, for example, exciton binding, double excitations, orbital relaxation, and polyradical character. A broad range of quantum-chemical methods is interfaced with libwfa via a uniform interface layer in the form of DMs. This contribution reviews the structure of libwfa and highlights its capabilities by several representative use cases.

This article is categorized under:

Software > Quantum Chemistry

Theoretical and Physical Chemistry > Spectroscopy

KEYWORDS

excited states, excitons, quantum chemistry, wavefunction analysis

1 INTRODUCTION

Open-shell and electronically excited species¹ are important in many areas of science, such as organic electronics,² chemical synthesis,³ and biology.⁴ A number of powerful quantum chemistry methods afford an efficient treatment of large molecules and accurate description of even the most intricate electronic structures. 1,5-10 However, the ability to produce accurate numbers alone is not sufficient—an important role of theoretical modeling is to also provide physical insight. Challenges toward obtaining such insight stem from technical issues, such as the sheer quantity of data produced and the difficulty of comparing results from different quantum chemistry methods, as well as from more fundamental issues, for example, the relationships between physical observables, many-body wavefunctions, and the molecular orbital framework. 11,12

Motivated by these problems and limitations, researchers have designed a number of excited-state analysis tools to provide compact visualization^{13–15} and quantitative analysis^{16–20} of excited-state processes. However, many of these tools were implemented only for specific use cases and selected quantum chemical methods, and were compatible only with some software packages. Hence, the design idea of libwfa was to provide a flexible, comprehensive, and transferable toolbox for excited-state analysis. libwfa affords a hierarchy of features of interconnected visual and quantitative analysis that illuminate excited-state properties from a variety of perspectives and allow for fully automated processing of excited state characters. The implemented methods rely on various types of density matrices (DMs), reduced objects whose mathematical properties are well documented.^{21,22} DMs provide a rigorous basis for extracting molecular orbital pictures and numerical descriptors from intricate correlated wave functions.^{12,23} DMs also allow one to connect the computed quantities with experimentally relevant observables by virtue of operator expectation values. Basing the analysis on DMs is convenient because it affords an ansatz-agnostic implementation, which is independent of the quantum chemistry method employed.

libwfa enables visualization of various densities and orbitals along with population analyses of the computed densities. An interface to the TheoDORE program²⁴ enables a fragment-based analysis²⁵ that can be used for an automatic excited-state assignment, for example, for interacting chromophores, pull systems, and transition-metal complexes. A complementary perspective is provided by a correlated electron-hole pair and a statistical analysis thereof, thereof, and the highlight dynamic charge-transfer effects in conjugated polymers, elucidate the diffuseness of Rydberg states, and to describe the nature of core-excited states. By providing various descriptors, libwfa facilitates the connection between many-body calculations and simple physical models of chemical bonding and excited states. For example, libwfa can be used to provide insight into phenomena, such as double excitations, and polyradical character, entanglement, entanglement, exciton binding and exchange repulsion, de-excitations, and polyradical character, and sheds new light onto Hückel theory and valence-bond theory. The formalism has been extended to electronically metastable states, spin-forbidden transitions and magnetic properties, and nonlinear optical phenomena.

This contribution presents libwfa from the end-user perspective, that is, for a researcher using an existing libwfa interface to solve scientific problems. For this reason, we focus on the physics these tools can reveal rather than technical details of the implementation. Toward this purpose, we first lay out the overall structure of libwfa and list the implemented analysis methods along with the key equations, highlighting their domain of applicability. We then present several use cases, which illustrate selected features of libwfa. These examples highlight unique capabilities of libwfa and illustrate functionality that is not accessible with TheoDORE and other available wavefunction analysis codes. We begin by discussing the lowest singlet $n\pi^*$ and $\pi\pi^*$ states of uracil and show how libwfa can be used to gain detailed insights into its oscillator strengths and excitation energies. As a second example, we have chosen (hexa)thiophene (a large π -conjugated system) to illustrate the utility of libwfa in understanding the differences between various quantum chemical methods (e.g., between ab initio methods and time-dependent density functional theory [TDDFT] with different exchange-correlation functionals). We then present an example of using libwfa to distill generalized El-Sayed's rules from correlated many-body wavefunctions of a magnetic iron complex. Our last example illustrates the extension of libwfa to the response DMs, which affords a molecular orbital description of nonlinear optical phenomena.

2 | FUNCTIONALITY AND PROGRAM STRUCTURE

libwfa is an open-source C++ library (distributed at github.com/libwfa), designed to provide an extensible platform for implementing analysis methods and to facilitate interfaces to quantum chemistry methods and programs. It provides a central interface layer connecting a wide range of quantum chemistry methods with a hierarchy of interconnected analysis methods. Figure 1 presents the structure of libwfa, along with a list of the implemented features. The overall workflow is sketched at the top of Figure 1. A libwfa job starts with a quantum-chemical excited-state computation (shown on the top left). A broad variety of methods can be used. For example, Q-Chem^{23,48} offers a variety of single-reference methods: algebraic diagrammatic construction (ADC),^{7,49} equation-of-motion coupled cluster (EOM-CC),^{6,10} and TDDFT, including various variants of these methods that do not conserve spin or particle number (i.e., spin-flipping,⁵⁰ ionizing or electron-attaching, etc). Alternatively, several multireference methods are available via OpenMolcas.^{51,52} multiconfigurational self-consistent field (MCSCF) and complete or restricted active space perturbation theory (CASPT2/RASPT2).⁵³ All what is required from any of these methods is transition and/or state DMs, which enables a uniform analysis and an ansatz-agnostic (i.e., independent on underlying wavefunction or density-functional

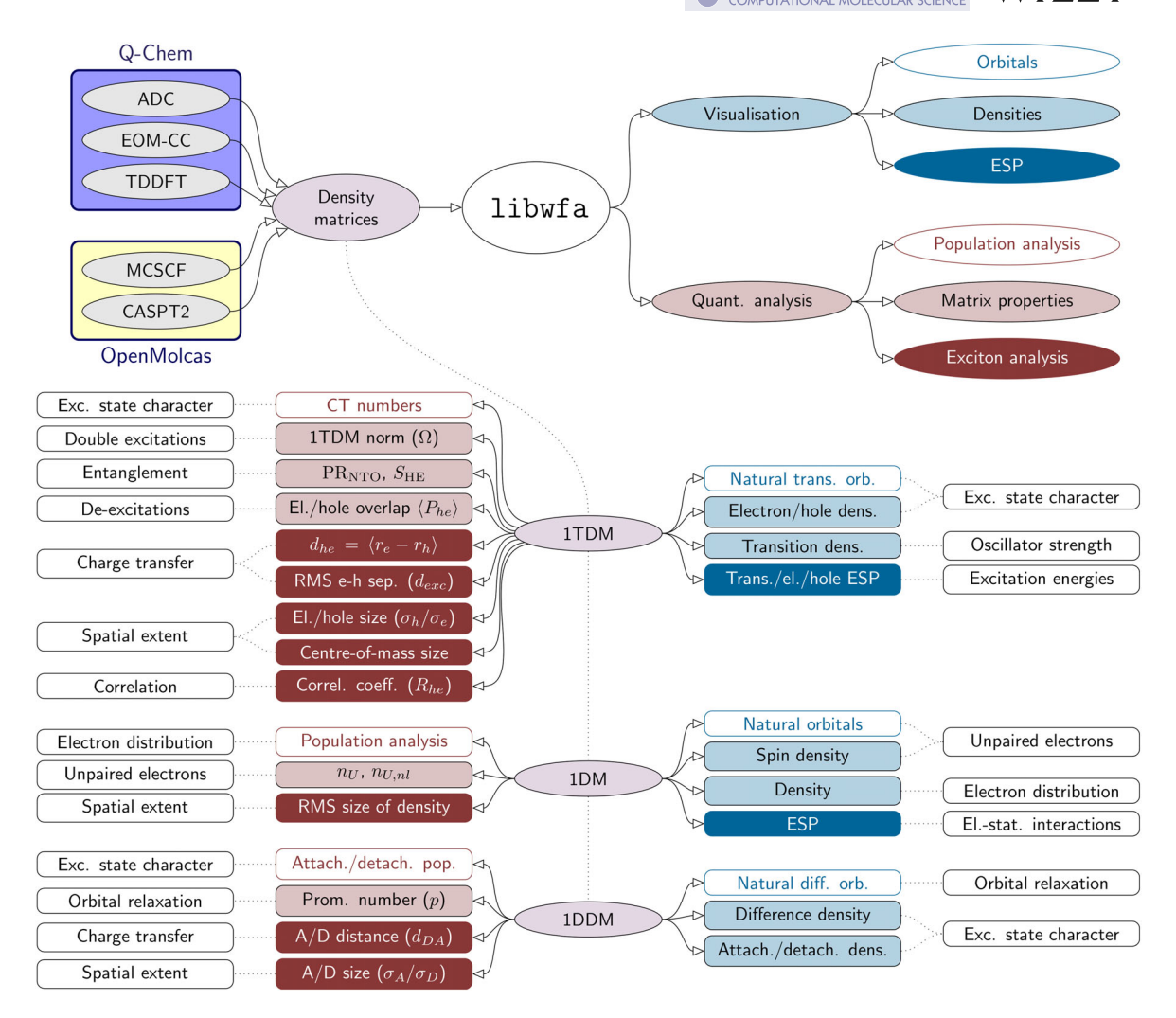


FIGURE 1 Structure of the wavefunction analysis library libwfa. *Top*: Workflow showing input from quantum chemistry programs on the left and various analysis outputs on the right. *Bottom*: Implemented analysis methods for the one-electron transition density matrix (1TDM), density matrix (1DM), and difference density matrix (1DDM); visualization methods to the right, quantitative analysis methods to the left. Perturbed 1TDMs can be passed instead of 1TDMs for the analysis of nonlinear optical properties

models) interface. The DMs are fed into libwfa, where they are used for a variety of analysis tasks. The main visualization tasks are concerned with (i) orbitals formed as eigenvectors or singular vectors of DMs, (ii) densities obtained as weighted sums over orbitals, and (iii) electrostatic potentials (ESPs) induced by these densities. These visualization tasks are complemented by quantitative analyses, classified into (iv) population analyses of one of the densities discussed above, (v) orbital-invariant matrix properties (norms, traces, etc) that describe the structure of the DMs, and (vi) expectation values computed by contracting the DMs with different integrals. All implemented analysis methods are ansatz-agnostic and invariant with respect to the molecular orbital (MO) expansion. The only partial exception concerns the population analyses methods (iv), which utilize the Mulliken or Löwdin style analysis and, therefore, require explicit knowledge of the underlying atomic orbital basis (but are still invariant to the MO expansion).

From a more technical viewpoint, Figure 1 highlights that libwfa provides the routines for the central analysis tasks (i–vi). These are implemented efficiently, as matrix operations. For its operation, libwfa requires the DMs and some other basic pieces of information depending on the type of analysis of interest, most importantly the molecular geometry, the definition of the basis functions, and the overlap and one-electron operator matrices (multipole moments). This information is not created by libwfa itself but is generated by the quantum chemistry program and supplied to libwfa via a suitable interface. In the case of Q-Chem, the interface proceeds by directly passing data pointers to libwfa whereas OpenMolcas writes all required data into an HDF5 file that is subsequently read by libwfa. This close integration of libwfa with quantum chemistry programs provides access to a variety of data, such as one-electron operator

integrals, non-standard response densities, and even two-electron integrals. libwfa also takes advantage of data-export utilities of the quantum chemistry program to which it is interfaced. Presently, the generation of MO coefficients in Molden format, cube files with data on a grid, and formatted checkpoint files are supported for the visualization tasks, shown at the top right of Figure 1. This close integration with quantum chemistry programs distinguishes libwfa from codes that simply post-process the outputs, such as the TheoDORE code.²⁴

Documentation on using the implemented features is provided within the user manuals of the Q-Chem and OpenMolcas program packages. In Q-Chem, the analysis is turned on by the "state_analysis = true" keyword and in OpenMolcas the analysis proceeds via the WFA module. An overview of the C++ code with all implemented modules and classes of libwfa is given in the Supporting Information.

The bottom part of Figure 1 shows the implemented methods, grouped in terms of the type of DM analysis, and indicates the connection to the relevant physical properties. libwfa considers three different types: the 1-electron transition density matrix (1TDM), density matrix (1DM), and difference density matrix (1DDM). Perturbed 1TDMs can be passed instead of 1TDMs for the analysis of nonlinear optical properties. For electronically metastable states described by non-Hermitian methods, ¹⁰ libwfa can be deployed to analyze the real and imaginary components of 1TDM. ⁴³ For spin-forbidden transition and magnetic properties, spinless 1TDMs are used. ⁴⁴

The central property for analysis is the 1TDM, formally defined as the two-body function

$$\gamma_{if}(r_{h}, r_{e}) = n \int \cdots \int \Psi_{i}^{*}(r_{h}, r_{2}, ..., r_{n}) \Psi_{f}(r_{e}, r_{2}, ..., r_{n}) dr_{2} ... dr_{n} = \sum_{pq} D_{pq}^{if} \phi_{p}(r_{h}) \phi_{q}(r_{e}), \tag{1}$$

where Ψ_i and Ψ_f are the wavefunctions of the initial (usually, ground) and final (e.g., excited) states, respectively. \mathbf{D}^{if} (which is also called 1TDM) is its matrix representation in the molecular orbital basis $\left\{\phi_p\right\}$:

$$D_{pq}^{\text{if}} = \langle \Psi_{\text{i}} | p^{\dagger} q | \Psi_{\text{f}} \rangle. \tag{2}$$

The 1TDM provides a mapping between the initial and final many-body wave-functions in terms of one-electron excitations:

$$|\Psi_{\rm f}\rangle = |\Psi_{\rm f}^{\rm S}\rangle + |\Psi_{\rm f}^{\rm DT\cdots}\rangle = \sum_{pq} D_{pq}^{\rm if} q^{\dagger} p |\Psi_{\rm i}\rangle + |\Psi_{\rm f}^{\rm DT\cdots}\rangle. \tag{3}$$

It, thus, provides a rigorous way of decomposing the wavefunction Ψ_f into singly (Ψ_f^S) and higher $(\Psi_f^{DT...})$ excited contributions with respect to Ψ_i . We also note (following Ref. 54) that the 1TDM yields the coefficients for maximizing the overlap between Ψ_f and Ψ_f^S for any such expansion.

Importantly, the 1TDM contains all essential information needed for computing one-electron transition properties, such as dipole or magnetic moments, angular momentum, and the leading contribution to non-adiabatic couplings.⁵⁵

For further analysis, the 1TDM can interpreted as an effective exciton wavefunction (cf. Refs. 56, 57), which describes the distribution of the correlated electron-hole pair via the coordinates r_e and r_h , respectively.^{23,30} A singular-value decomposition of \mathbf{D}^{if} yields the most compact description of the exciton wavefunction in terms of hole and electron orbital pairs

$$\gamma_{\rm if}(r_{\rm h}, r_{\rm e}) = \sum_{\rm v} \sigma_{\rm K} \widetilde{\phi}_{\rm K}^{\rm h}(r_{\rm h}) \widetilde{\phi}_{\rm K}^{\rm e}(r_{\rm e}), \tag{4}$$

where σ_K are singular values and $\widetilde{\phi}_K^h(r_h)$ and $\widetilde{\phi}_K^e(r_e)$ are called natural transition orbitals (NTOs). NTOs provide a quantitative link between many-body wave-functions and molecular orbital theory. As per Equation (1), once the 1TDMs are computed, the details of many-body wavefunctions and orbital representation become irrelevant, which provides a basis for an unbiased and uniform analysis of the underlying electronic structure.

Visualization methods for the 1TDM are shown on the right in Figure 1; they comprise plotting NTOs and the electron/hole densities (defined as weighted sums over NTOs). Both are useful for assigning the character of the excitation. Transition densities provide an insight into experimental observables, for example, the polarization and brightness

of transitions. libwfa also affords the computation of ESPs of the electron, hole, and transition density, which allows to visualize different electrostatic interactions that contribute to the excitation energies.¹¹

Whereas visualization techniques are useful for a quick intuitive assignment of state character, it is often desirable to obtain a quantitative analysis for, for example, automation of large-scale calculations, achieve machine-learning applications, or the detection of more subtle details. The descriptors, available for this purpose, are shown on the left in Figure 1.

To illustrate the concept of descriptors, we begin with the charge transfer (CT) numbers, introduced in Ref. 25 following ideas from Refs 17, 61. The system is first divided into several chemically meaningful fragments. Subsequently, for any pair of fragments A and B, the CT numbers are computed as an integral of the form

$$\Omega_{AB} = \int_{A} \left[\int_{B} |\gamma_{if}(r_h, r_e)|^2 dr_e \right] dr_h, \tag{5}$$

giving the mutual probability that the hole is on fragment A while the electron resides on B. Equation (5) highlights that the CT numbers can be computed directly from the 1TDM without reference to the orbitals. Note, however, that the formal integration basins defining the fragments A and B have to be defined; libwfa allows to do so via the Mulliken- or Löwdin-style population analyses. The CT numbers allow one to describe the transition in terms of the local and CT contributions; they have been used to assign excited-state character for, for example, interacting chromophores, ²⁶ push–pull systems, ^{27,28} and transition-metal complexes. ²⁹ In practice, the analysis proceeds via a two-step procedure where libwfa computes the CT numbers with respect to individual atoms and the summation over fragments along with further processing is done by the separate TheoDORE program. ²⁴

In the second category, shown in light red in Figure 1, libwfa computes a number of 1TDM descriptors as matrix properties, such as eigenvalues and norms. These properties are independent of the shape of the underlying orbitals describing the properties of the wavefunctions on a fundamental level. The first such property is the squared 1TDM norm^{23,55}

$$\Omega = \int \left| \left| \gamma_{if}(r_h, r_e) \right|^2 dr_e dr_h = \left\| \mathbf{D}^{if} \right\|^2.$$
 (6)

By left-multiplying Equation (3) with $\langle \Psi_f |$ and assuming Ψ_f to be normalized, one finds

$$1 = \langle \Psi_f | \Psi_f^S \rangle + \langle \Psi_f | \Psi_f^{DT...} \rangle = \Omega + \langle \Psi_f | \Psi_f^{DT...} \rangle, \tag{7}$$

that is, Ω amounts to the overlap of the final wavefunction Ψ_f with the singly excited (with respect to Ψ_i) contributions Ψ_f^S (or, in other words, provides the collective weight of singly excited configurations). If Ω is exactly 1, then the excited state can be understood as being purely singly excited with respect to the (correlated) ground state. Conversely, values significantly lower than 1 indicate the involvement of higher excitations. For practical applications, it should be pointed out that the 1TDM analysis only considers the singly excited contributions and can, thus, only provide a comprehensive picture if Ω is sufficiently close to 1.

In addition, libwfa computes two measures of entanglement, which report on the inherent multiconfigurational character of the transition,³⁷ the NTO participation ratio (PR_{NTO}) and the entanglement entropy between hole and electron (S_{HE})

$$PR_{NTO} = \frac{\Omega}{\sum_{V} \sigma_{K}^{4}}, S_{HE} = -\sum_{K} \sigma_{K}^{2} \log_{2} \sigma_{K}^{2},$$
(8)

where the σ_K are the NTO singular values. Both PR_{NTO} and $S_{\rm HE}$ are equal to 1 for states that can be described by a single orbital transition and assume higher values if several configurations are involved. (Care should be taken to consistently handle spin-adapted and non-spin-adapted calculations, as discussed in Refs. 38 and 12). Finally, the deexcitation character is quantified by measuring the non-nilpotency of the 1TDM by computing the overlap between electron and hole, formally defined as the expectation value of the electron-hole permutation operator $\langle P_{\rm he} \rangle$. ¹¹

A more extended set of quantitative analysis tools is built around the computation of expectation values of the effective exciton wavefunction³⁰ defined as

$$\langle \widehat{O} \rangle_{\text{ex}} = \frac{\langle \gamma_{\text{if}} | \widehat{O} | \gamma_{\text{if}} \rangle}{\Omega} = \frac{1}{\Omega} \sum_{K,L} \sigma_K^* \sigma_L \langle \widetilde{\phi}_K^h | \widehat{O} | \widetilde{\phi}_L^e \rangle. \tag{9}$$

The resulting quantities, which are called exciton descriptors, provide a way to quantitatively describe characters of excited states and to connect with intuitive physical models. The right-hand-side of Equation (9) illustrates that these descriptors cannot be computed from the individual NTO pairs (except for a trivial case when only one NTO pair contributes to the excitation) and are affected by the cross terms. It is by virtue of these cross terms that the analysis can differentiate between pairs of states with identical NTOs, for example, excitonic and charge-resonance states in dimers³⁰ or the B_{3u}^- (B_b) states of naphthalene. B_{3u}^- (B_b) and B_{3u}^+ (B_b) states of naphthalene.

Based on these expectation values, libwfa offers a detailed description of the electron-hole distribution using various multipole moments. First, charge transfer is quantified via the linear (d_{he}) and root-mean-square (d_{exc}) electron-hole separations

$$d_{\text{he}} = \langle r_{\text{e}} - r_{\text{h}} \rangle_{\text{ex}} , d_{\text{exc}} = \sqrt{\langle (r_{\text{e}} - r_{\text{h}})^2 \rangle_{\text{ex}}}$$
 (10)

The spatial extent of the excitation is quantified via the root-mean-square size of the hole (σ_h), electron (σ_e), and the formal center-of-mass σ_{CM} .

$$\sigma_{h/e} = \sqrt{\langle r_{h/e}^2 \rangle_{ex} - \langle r_{h/e} \rangle_{ex}^2}, \quad \sigma_{CM} = \sqrt{\langle \left(\frac{r_h + r_e}{2}\right)^2 \rangle_{ex} - \left\langle \frac{r_h + r_e}{2} \right\rangle_{ex}^2}$$
(11)

Finally, a correlation coefficient

$$R_{\text{he}} = \frac{\langle r_{\text{h}} r_{\text{e}} \rangle - \langle r_{\text{h}} \rangle \langle r_{\text{e}} \rangle}{\sigma_{\text{h}} \sigma_{\text{e}}} \tag{12}$$

describes whether, on average, electron and hole attract or avoid each other dynamically.³¹

libwfa also supports analyses of the 1DM ($\gamma_{\rm ff}$), which is defined in analogy to Equation (1) but with equal bra and ket states. A number of standard visualization methods are provided, for example, the natural orbitals, the spin- and overall electron density along with its ESP, and a population analysis. For example, libwfa computes measures for unpaired electrons $n_{\rm U}$ and $n_{\rm U,nl}$, ⁶² which are convenient for discussing the electronic structure of polyradical systems. ^{39,40} Finally, the root-mean-square size of the density ⁵¹ is computed

$$\sigma_{\rho} = \sqrt{\frac{\langle r^2 \rangle - \langle r \rangle^2}{N}} \tag{13}$$

where N is the number of electrons and $\langle . \rangle$ refers to a usual operator expectation value. σ_{ρ} allows to quantify the diffuseness of a state. Although being conceptually similar to simply using the $\langle r^2 \rangle$ value, this descriptor provides a value that is of the order of the size of the molecule and independent of the coordinate origin.

Analyses of the 1DDM, defined as the difference $\gamma_{\rm ff} - \gamma_{\rm ii}$ for a given pair of *initial* and *final* states, are centered around the attachment/detachment densities, ¹⁴ which, along with the difference density, provide a convenient means for representing excited-state character in a compact way. The eigenvectors of the 1DDM, the natural difference orbitals (NDOs), are identical to NTOs for the CIS ansatz (for the transitions between the ground and excited states) and, therefore, are often similar to NTOs for the transitions with dominant singly excited character. Yet, the differences between NTOs and NDOs can be used to gain detailed insight into orbital relaxation effects ^{34,36,51} or multiple excitation characters, neither of which are captured by the 1TDM. The total number of attached/detached electrons, also known as the promotion number p serves as a measure of the total number of electrons rearranged, either during the primary

excitation process or as secondary orbital relaxation. In addition, some exciton properties, most notably a linear charge transfer distance d_{DA} and a root-mean-square size of the A/D densities (σ_A , σ_D), can be computed serving a similar purpose as the analogous 1TDM descriptors. However, only a reduced set of descriptors is available as it is not possible to construct a correlated two-body function in analogy to Equation (1). Finally, we note that the 1DDM can be computed between any pair of wavefunctions expressed over the same set of atomic orbitals and is, therefore, readily applicable for states with different numbers of electrons,⁵¹ providing similar information as the Dyson orbitals.¹² The 1DDM can even be obtained from completely independent computations as long as the 1DMs or natural orbitals are stored.⁶³

3 | REPRESENTATIVE EXAMPLES

3.1 | Physical insight into excitation processes

Figure 2 shows a typical application of libwfa, exemplified by the visualization of the lowest singlet $n\pi^*$ and $\pi\pi^*$ states of uracil. The example shows how libwfa can extend a simple assignment of state character to a deeper understanding of excited-state energies and properties. The NTOs, shown at the top, provide a compact and unique representation of the transition, which is orbital-invariant and ansatz-agnostic and provides a direct connection to spectroscopic observables (e.g., the transition dipole) via matrix elements between them. In addition to revealing the main character of the excitations $(n\pi^* \text{ vs. } \pi\pi^*)$, NTOs provide a more detailed physical picture. They show, for example, that the acceptor π^* -orbital possesses the same nodal structure in both cases but is polarized slightly differently, thus, indicating primary orbital relaxation of this orbital to accommodate the respective shape of the excitation hole. libwfa offers the opportunity to dig even deeper, to better understand how the shapes of the orbitals are related to energies and other physical observables. For example, at the bottom of Figure 2, the transition density is shown, which is responsible for the optical brightness of the transition. For a transition dominated by a single NTO pair, the transition density is represented by the product of the two dominant NTOs.³⁴ For the $n\pi^*$ state the transition density is a product of two perpendicular p-type orbitals, giving rise to a d-orbital shape, whereas for the $\pi\pi^*$ state the transition density is a product of collinear p-orbitals. The transition dipole moment, which is the dipole moment of the transition density, is depicted by a green arrow pointing from the predominantly blue part to the red part. The transition dipole moment almost vanishes for the $n\pi^*$ state, as expected from the quadrupolar shape of the transition density (which is, in turn, caused by the shapes of the NTOs). In contrast, the $\pi\pi^*$ state has a sizeable transition dipole moment parallel to the molecular plane.

We can also use this representation to learn about excitation energies. The excitation energies can be understood in terms of orbital energy differences corrected by the Coulomb and exchange terms. The Coulomb term, sometimes called exciton binding energy, can be understood as a Coulomb attraction within the correlated electron—hole pair. In simple cases, this corresponds to a static attraction between the electron and hole densities, whereas in general also correlation effects can play a role, for example, when differentiating between excitonic and charge-resonance states in

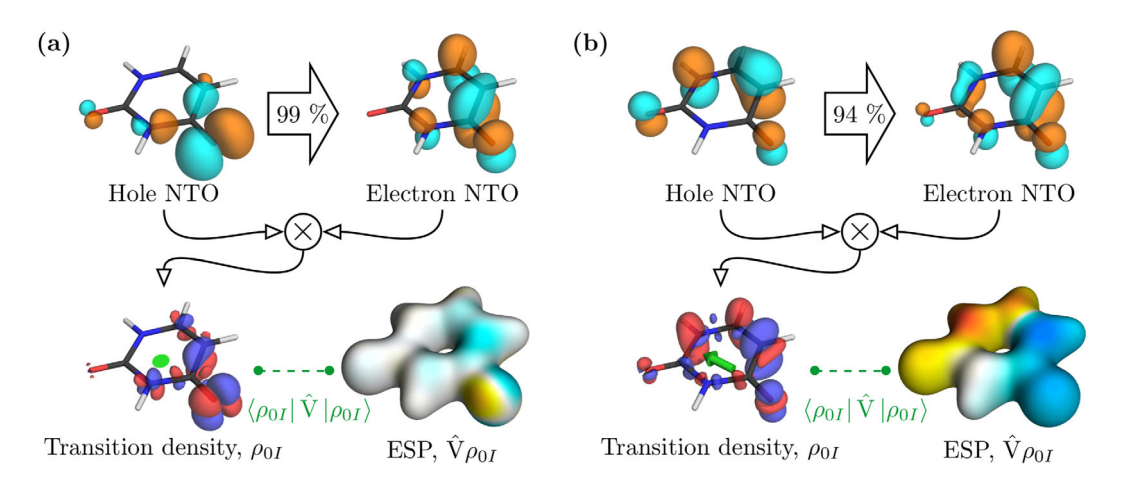


FIGURE 2 Analysis of the lowest (a) $n\pi^*$ and (b) $\pi\pi^*$ singlet excited states of uracil at the ADC(2) level of theory. *Top*: Dominant pair of natural transition orbitals and its contribution to the excitation. *Bottom*: Transition density with transition moment and ESP induced by the transition density (modified with permission from Ref. 11. Copyright 2020, the Owner Societies)

dimers³⁰ or when studying various excitonic bands in conjugated polymers.⁶⁵ The energy gap between singlets and triplets arises due to the exchange term, which destabilizes the singlet and can be described as the repulsion of the transition density with itself.¹¹ This term can also be interpreted as an overlap of the transition density with the ESP induced by it and we, therefore, also present the ESP in Figure 2. For the $n\pi^*$ state, one finds that the ESP almost vanishes leading to minuscule exchange repulsion. For the $n\pi^*$ state, a significant repulsion is found in line with the large gap between the lowest singlet and triplet $n\pi^*$ states computed for uracil.¹¹ Finally, a deeper analysis of the σ contributions involved in the $n\pi^*$ state shows that these have the effect of reducing the magnitude of the transition ESP and hence lower the energy of the state while also lowering the transition moment.¹¹ This last analysis illustrates that even seemingly simple $n\pi^*$ states have an intricate dependence on σ contributions and not treating them correctly causes errors in energies as well as oscillator strengths, a phenomenon widely discussed in the literature.⁶⁶⁻⁶⁸

3.2 | Method comparison

Benchmarking excited-state methods is a crucial task in quantum chemistry, which is used to assess the accuracy and scope of existing methods and to develop the path toward new ones. ^{69,70} Most often, benchmarking is based on excitation energies, which are experimentally accessible physical observables. However, relying only on the energies can be misleading as a spurious agreement may happen, despite an incorrect description of the wavefunctions, making the method unreliable for predicting other aspects of the photophysics. Moreover, even if a disagreement between methods is found, it is often hard to pin down the reason based on the energies alone. libwfa is particularly suitable for benchmarking and comparing different methods ^{40,71,72} due to the wide range of analysis methods implemented and the fact that these methods are based on DMs, which represent a uniform and ansatz-agnostic description of excited states.

Conjugated polymers and, more generally, large conjugated π -systems, represent a class of molecules for which many standard density functionals are surprisingly inaccurate even for systems without apparent charge transfer. Figure 3 illustrates this issue for the hexa(thiophene) molecule. Correlated ab initio methods, ADC(2) and EOM-CCSD, provide the reference values. TDDFT (within the Tamm–Dancoff approximation) was performed using the BLYP, B3LYP, and CAM-B3LYP functionals to represent semi-local, hybrid, and range-separated hybrid functionals, respectively. Finally, configuration interaction with single excitations (CIS) was used to represent the

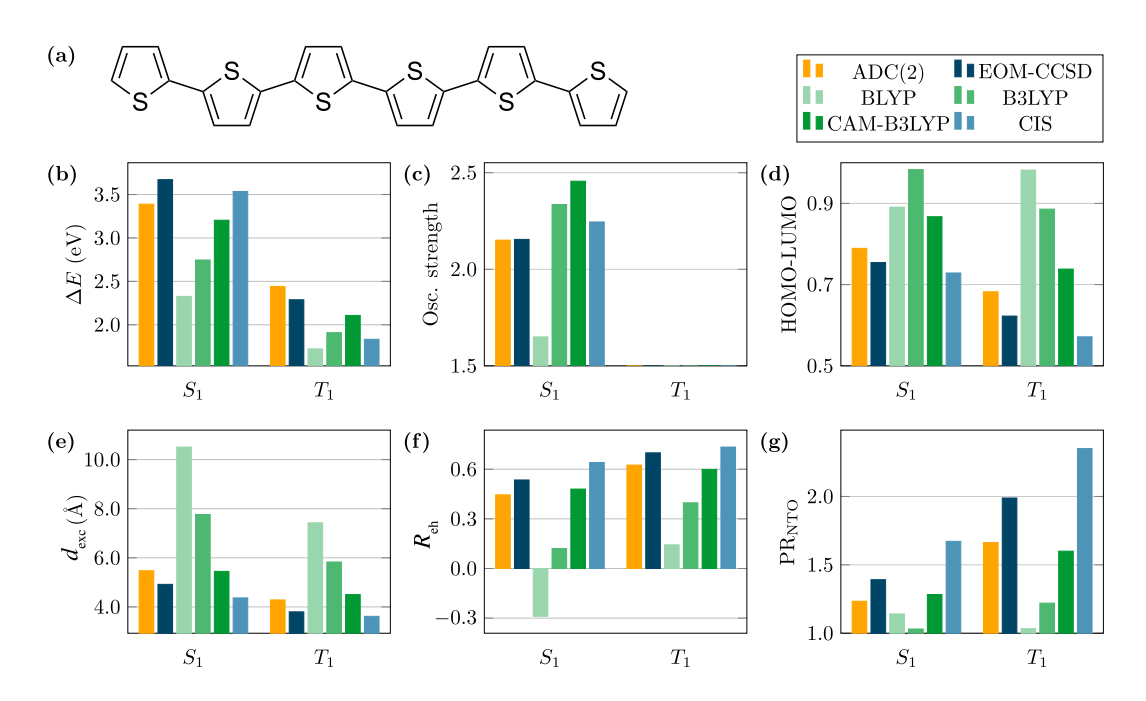


FIGURE 3 Analysis of the S_1 and T_1 excited states of hexa(thiophene) using various electronic structure methods: (a) molecular structure of hexa(thiophene), (b) excitation energies, (c) oscillator strengths, (d) weight of the HOMO–LUMO transition, (e) root-mean-square electron–hole separation, (f) electron–hole correlation coefficient, and (g) NTO participation ratio

limiting case of 100% unscreened Hartree–Fock exchange. Quantities that are routinely available are shown in Figure 3b–d whereas specific quantities computed by libwfa are shown in Figure 3e–g. Starting with the excitation energies (Figure 3b), we observe striking differences between the methods: the computed S_1 energies range from only 2.33 eV (BLYP) up to 3.67 eV (EOM-CCSD) and also the T_1 energies are quite widely distributed, between 1.72 eV for BLYP and 2.44 eV for ADC(2). Oscillator strengths are shown in Figure 3c revealing substantial discrepancies following similar trends as found for the excitation energies. Inspection of the molecular orbitals involved shows that S_1 and T_1 are dominated by the HOMO–LUMO transition. Figure 3d highlights that the HOMO–LUMO transition always contributes with more than 50% but it also shows conspicuous differences between the methods in terms of its weight. The role of libwfa can now be seen as a tool for revealing the missing contributions beyond the HOMO–LUMO transition.

TDDFT excitation energies increase in the BLYP < B3LYP < CAM-B3LYP series, that is, according to increasing Hartree-Fock exchange, suggesting that the issue is related to self-interaction errors leading to well-known problems of TDDFT with CT states.⁷⁷ It may appear contradictory to talk about CT in a system with perfect inversion symmetry not possessing donor or acceptor groups. Indeed, the more appropriate physical picture is that of a correlated electron-hole pair^{56,57} whose apparent Coulomb binding energy depends on the methods used.^{32,78} Such dynamic binding effects can be elucidated within libwfa using the root-mean-square electron-hole separation or exciton size $d_{\rm exc}$, as defined in Equation (10).³⁰ Results for $d_{\rm exc}$ are presented in Figure 3e highlighting that these vary strongly between the methods. Generally, an inverse correlation between ΔE and $d_{\rm exc}$ is found with the largest exciton sizes found for BLYP and the smallest ones for CIS. A complementary perspective is provided via the correlation coefficient $R_{\rm he}$, defined in Equation (12), which analyses the mutual distribution of the electron and hole quasiparticles. A positive value for R_{he} is obtained for a bound exciton where electron and hole move in a concerted fashion whereas a negative value indicates that they avoid each other dynamically. Consistently with the picture of a bound electron-hole pair present in the conjugated polymer, 56,57 we find that the $R_{\rm he}$ values are positive in almost all cases. Considering TDDFT and CIS, one finds that R_{he} increases with the amount of Hartree-Fock exchange included and that only CAM-B3LYP and CIS are in a reasonable agreement with the correlated ab initio reference values. Notably, the S_1 state as computed with BLYP has a negative R_{he} value, thus, indicating even incorrect qualitative behavior showing dynamic repulsion rather than attraction, failing to form a bound state of the exciton (cf. Ref. 78).

Finally, it is interesting to compare spatial correlation, as reported by the R_{he} value, with the intrinsic multiconfigurational character of the state. Naively, the multi-configurational character can be quantified by the weight of the dominant configuration expressed in terms of canonical orbitals, as shown in Figure 3d. However, this description is not orbital invariant and does not represent the intrinsic character of the transition. In contrast, libwfa provides 1TDM and 1DM based descriptors that are orbital-invariant and are uniquely defined. The NTO participation ratio (PR_{NTO}), defined in Equation (8), is one such descriptor. In the present case, one finds a reasonable correspondence between the weight of the HOMO–LUMO transition and PR_{NTO}, that is, Figure 3d,g, but this correspondence often deteriorates in more complicated cases, for example, when larger basis sets are employed (see examples in Refs. 12 and 15). More importantly, one also finds a good correlation between R_{he} and PR_{NTO} indicating a relation between spatial correlation and multi-configurational character.

A number of studies have employed libwfa to shed light on the phenomena discussed above. The trends relating $d_{\rm exc}$ and $R_{\rm he}$ to the amount of Hartree–Fock exchange were found across a wide range of conjugated polymers and functionals. The underlying physics were discussed in more detail in Ref. 11. A direct visualization of the correlated electron–hole pair was presented in Ref. 42.

3.3 | NTOs of spin-forbidden transitions: El-Sayed's rules

The concept of NTOs was recently generalized⁴⁴ to characterize spin-forbidden transitions and magnetic properties. The essential advance here was to employ the spinless 1TDM, which, by virtue of the Wigner–Eckart theorem, can be used to compute spin–orbit couplings between all multiplet components.⁸¹ This circumvents the need to compute and analyze multiple 1TDMs (e.g., for the three M_S components of a triplet state) and also eliminates arbitrariness due to the dependence of the individual spin–orbit coupling matrix elements on the molecular orientation. Just as regular NTOs are directly related to the experimental observables (e.g., transition dipole moments between the two many-body states can be expressed in terms of dipole moment matrix elements between hole and particle NTOs), these spin–orbit NTOs afford interpretation of the computed property (spin–orbit coupling constant, barriers for spin-reorientation, etc)

in terms of molecular orbital theory. For example, this analysis provides a quantitative basis for El-Sayed's rules, ⁸² which posit that large SOC requires orbital torque because of the non-diagonal structure of the angular momentum operator (see left panel of Figure 4). The original El-Sayed rules ⁸² explained why intersystem crossings involving an orbital flip (e.g., ${}^{1}\pi\pi^* \rightarrow {}^{3}n\pi^*$) occur much more readily than transitions between states of the same orbital character (e.g., ${}^{1}\pi\pi^* \rightarrow {}^{3}\pi\pi^*$). The right panel of Figure 4 shows spin-orbit NTOs between the interacting multiplets in two single-molecule magnets with an Fe(II) centre. Spin-orbit coupling splits the otherwise degenerate components of the quintet (d^6) state and creates a barrier U for spin reorientation. The calculations ⁸⁰ yield barriers that differ by a factor of two. The computed NTOs reveal that the spin-orbit interaction involves different M_s components of iron's d-orbitals, which leads to large differences in the change of angular momentum ($\Delta L \approx 1$ vs. $\Delta L \approx 2$), and, consequently, in the magnitude of the spin-orbit couplings and U. This is an example of how an intuitive molecular orbital picture of the underlying physical phenomenon can be rigorously distilled from highly correlated wavefunctions.

3.4 | Nonlinear spectroscopic properties

Many important spectroscopies, for example, two-photon absorption (2PA), sum-frequency generation (SFG), resonant inelastic X-ray scattering (RIXS), operate in nonlinear regimes, and the underlying spectroscopic signal cannot be expressed as a single matrix element between the initial and final state; rather, the cross-sections are expressed as sum over all states of the system. For example, the *xy*-component of the 2PA transition moment is

$$M_{xy}^{f \leftarrow i}(\omega_x) = -\sum_{n} \left(\frac{\langle \Psi_f | y | \Psi_n \rangle \langle \Psi_n | x | \Psi_i \rangle}{\Omega_{ni} - \omega_x} + \frac{\langle \Psi_f | x | \Psi_n \rangle \langle \Psi_n | y | \Psi_i \rangle}{\Omega_{nf} + \omega_x} \right), \tag{14}$$

where $\Omega_{\rm ni}$ is the energy difference between states n and i. The frequencies of the two absorbed photons (polarized along x- and y-directions) are given by ω_x and ω_y such that $\omega_x + \omega_y = \Omega_{\rm fi}$. Equation (14) makes it clear that the simple NTOs computed for the 1TDM connecting the initial and final states do not map into the observable and cannot explain the magnitude of the transition moments. To overcome this problem, Equation (14) may be rewritten by formally subsuming the summation within the respective ket and bra states

$$M_{xy}^{f \leftarrow i}(\omega_x) = -\langle \Psi_f | y | \sum_n \Psi_n \frac{\langle \Psi_n | x | \Psi_i \rangle}{\Omega_{ni} - \omega_x} \rangle - \langle \sum_n \frac{\langle \Psi_f | x | \Psi_n \rangle}{\Omega_{nf} + \omega_x} \Psi_n | y | \Psi_i \rangle = -\langle \Psi_f | y | X_i^{\omega_x} \rangle - \langle \widetilde{X}_f^{\omega_x} | y | \Psi_i \rangle. \tag{15}$$

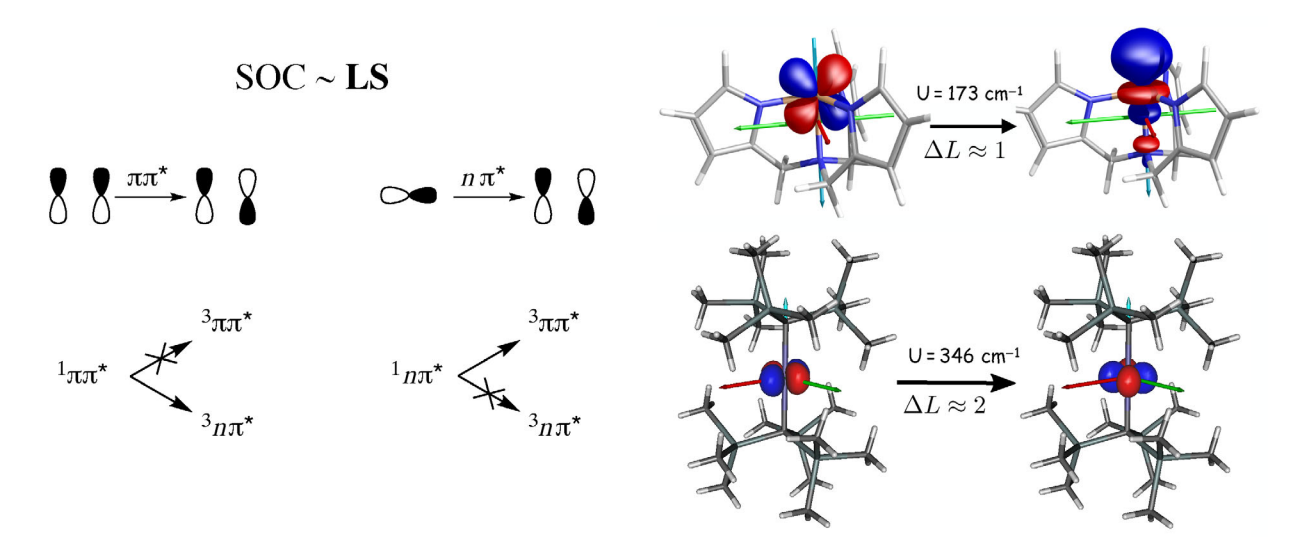


FIGURE 4 *Left*: Original El-Sayed's rules explain trends in intersystem crossing rates in terms of molecular orbitals. *Right*: SOC NTOs computed using EOM-EA-MP2 wavefunctions for Fe(II) single-molecule magnets explain the difference in the computed spin-reorientation barrier in terms of angular momentum change of the orbitals⁸⁰

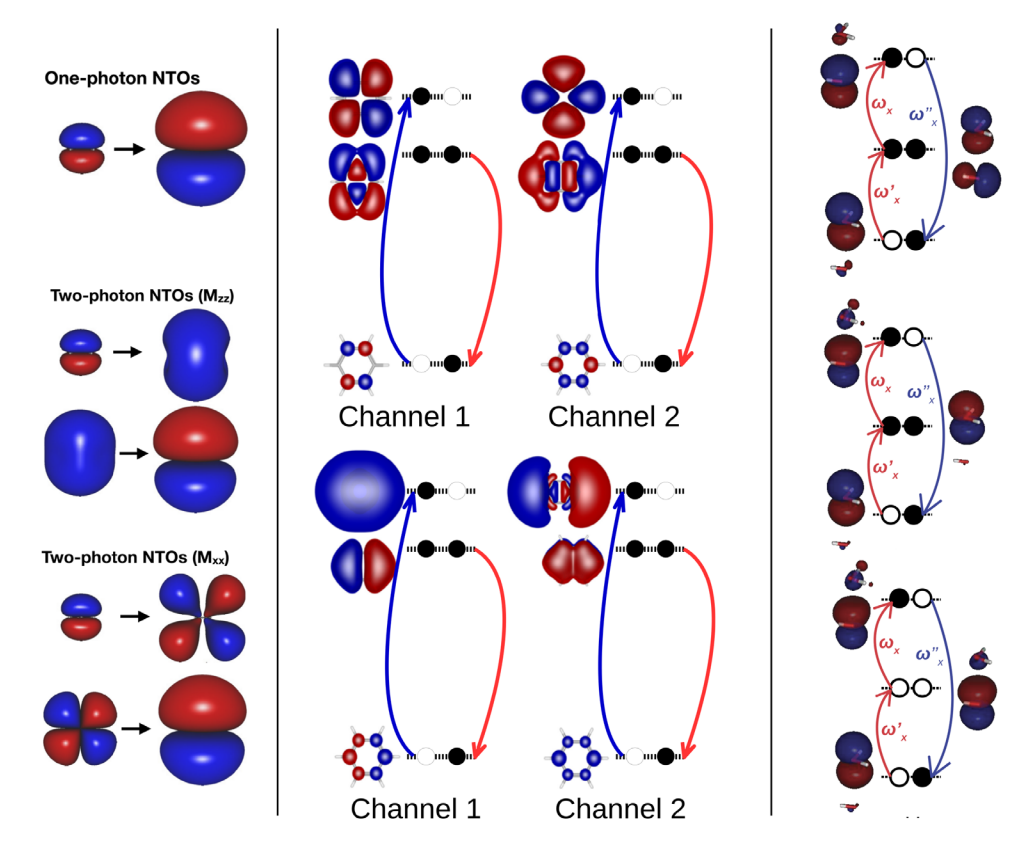


FIGURE 5 Left: NTOs characterizing one and two photon transition $\pi \to Ry(p_z)$ in ethylene (reproduced with permission from Ref. 45; copyright American Chemical Society, 2017). Centre: Dominant orbital channels for two different RIXS transitions (XA_g \to 13B_{2g} and XA_g \to 1B_{2g}) in benzene (reproduced with permission from Ref. 46; copyright American Institute of Physics, 2020). Right: Important orbital channels for a hemi-bonded OH + H₂O complex in the SFG process (reproduced with permission from Ref. 47; copyright American Institute of Physics, 2021)

The right-hand-side of Equation (15) defines the effective response states $X_i^{\omega_x}$ and $\widetilde{X}_f^{\omega_x}$, which are formally constructed as a sum over all excited states of the system, and in practice computed via auxiliary response equations. ^{83,84} The physical meaning of the response states is that they describe the first-order response ⁸⁵ of the wavefunction to the perturbation with frequency ω_x . The response states assimilate the contributions from all real excited states of the system and, thus, provide concrete meaning to the so-called "virtual states", which are commonly invoked in nonlinear spectroscopies.

This strategy was used to implement the response NTOs (or NOs) for 2PA,⁴⁷ RIXS,⁴⁶ and second dipole hyperpolarisability (which also features second-order response states along with first-order response states).⁴⁷ Figure 5 shows three examples. The left panel illustrates the nature of virtual states in the $XA_g \to 2A_g$ 2PA transition in ethylene using degenerate photons.⁴⁵ The regular NTOs (shown on top) describe this transition as $\pi \to Ry(p)$, but offer no insight into the virtual state and do not explain the dependence of the cross-section on the polarization of the two photons or their energies. The response NTOs for the M_{zz} moment reveal a Ry(s)-like virtual state, which is found both for the $\Psi_i \to \widetilde{X}_f^{\omega_x}$ and $X_i^{\omega_x} \to \Psi_f$ transitions. Conversely, the response NTOs for M_{xx} reveal a Ry(d) or π^* -like virtual state, which, again, emerges both from the initial and final response states. The middle panel of Figure 5 shows RIXS NTOs for two different transitions in benzene ($XA_g \to 13B_{2g}$ and $XA_g \to 1B_{2g}$), illustrating that each transition comprises two orbital channels. Here, we have used the damped version of response theory to compute the auxiliary response states: the near-resonance and off-resonance orbital information is then encoded in the imaginary and real components of complex-valued response DMs, respectively. Finally, the right panel of Figure 5 shows three orbital channels involved in the SFG process in a hemi-bonded OH + H₂O complex.⁴⁷ In this example, the SFG process is one-photon resonant with the $XA \to 3A$ transition. The response NOs reveal the contributions of both resonant ($XA \to 3A$, local excitation) and nonresonant ($XA \to 4A$, charge-transfer excitation) channels. The important SFG orbital

 $\text{channels thus are: } p_x(\mathrm{H}_2\mathrm{O}) \overset{\omega_x'}{\to} \sigma(\mathrm{OH}^\cdot) + p_x(\mathrm{H}_2\mathrm{O}) \overset{\omega_x}{\to} p_x(\mathrm{OH}^\cdot) \overset{-\omega_x''}{\to} p_x(\mathrm{H}_2\mathrm{O}), \ p_x(\mathrm{H}_2\mathrm{O}) \overset{\omega_x'}{\to} p_x(\mathrm{H}_2\mathrm{O}) \overset{\omega_x}{\to} p_x(\mathrm{OH}^\cdot) \overset{-\omega_x''}{\to} p_x(\mathrm{H}_2\mathrm{O}), \\ \text{and } p_x(\mathrm{H}_2\mathrm{O}) \overset{\omega_x'}{\to} p_x(\mathrm{OH}^\cdot) \overset{\omega_x}{\to} p_x(\mathrm{OH}^\cdot) \overset{-\omega_x''}{\to} p_x(\mathrm{H}_2\mathrm{O}). \\ \end{aligned}$

4 | CONCLUSIONS AND OUTLOOK

We presented an overview of the wavefunction analysis library libwfa. libwfa provides a variety of interconnected analysis tools that can be uniformly and easily applied for different quantum chemical methods and programs. It affords a comprehensive and easy-to-use analysis toolkit for practitioners of excited-state quantum chemistry, which allows users to obtain the most information out of modern excited-state computations. libwfa facilitates analysis tasks and provides deep insights into the underlying physics and chemistry. We described the overall structure and the implemented methods and illustrated the applicability of libwfa by selected case studies. The uracil example highlighted how these tools augment simple excited-state character assignment by more detailed insight into physical observables, such as energies and oscillator strengths. By using (hexa)thiophene, we have shown how exciton analyses can provide detailed insight into the surprising failures of DFT. The properties of (hexa)thiophene were illustrated from the perspective of a correlated electron-hole pair as well as in terms of multiconfigurational character, obtaining a consistent picture regarding different exciton binding strengths for the different methods. The example of single-molecule magnets illustrated the utility of NTOs in distilling El-Sayed's rules from high-level calculations. Finally, we have shown how the concepts of NTOs and 1TDMs can be generalized to describe nonlinear optical phenomena by utilizing response theory.

In the future, we plan to increase the scope of phenomena that can be studied with libwfa to, for example, double excitations, excited-state aromaticity, ⁸⁶ nondynamic correlation, spin correlators, ⁸⁷ and extensions to two-body Dyson orbitals. ⁸⁸ To connect with physical models, we plan to enable an intuitive graphical energy decomposition analysis of excited states. ^{11,64,89} Finally, extending the interface to more quantum-chemical methods and software packages will increase the scope in terms of molecular systems and phenomena that can be studied. We welcome new developers who wish to add features to libwfa or create new interfaces.

ACKNOWLEDGMENTS

We are grateful for various contributions to the code by Dr Michael Wormit, Dr Stefanie A. Mewes, Benjamin Thomitzni, Dr Feng Chen, Patrick Kimber, Dr Kaushik D. Nanda, Dr Pavel Pokhilko, and Dr Wojtek Skomorowski. The development of libwfa has profited from discussions with a number of colleagues. FP wants to specifically thank Prof. Hans Lischka, Prof. Irene Burghardt, and Dr Jan-Michael Mewes for discussions during the early stages of the project. Anna I. Krylov wants to thank Prof. Anatoly Luzanov for many stimulating discussions. Anna I. Krylov acknowledges support from the National Science Foundation (CHE-1856342, for response NTOs) and the Department of Energy (DE-SC0018910, for spin-orbit NTOs).

CONFLICT OF INTEREST

Anna I. Krylov is the president and a part-owner of Q-Chem, Inc.

AUTHOR CONTRIBUTIONS

Felix Plasser: Conceptualization (lead); formal analysis (lead); software (lead); writing – original draft (lead); writing – review and editing (equal). **Anna I. Krylov:** Conceptualization (equal); software (equal); writing – original draft (equal); writing – review and editing (equal). **Andreas Dreuw:** Conceptualization (equal); software (equal); writing – review and editing (equal).

DATA AVAILABILITY STATEMENT

Data sharing is not applicable to this article as no new data were created or analyzed in this study.

ORCID

Felix Plasser https://orcid.org/0000-0003-0751-148X

Anna I. Krylov https://orcid.org/0000-0001-6788-5016

Andreas Dreuw https://orcid.org/0000-0002-5862-5113



RELATED WIRES ARTICLES

Q-Chem: An engine for innovation

adcc: A versatile toolkit for rapid development of algebraic-diagrammatic construction methods

Gator: A Python-driven program for spectroscopy simulations using correlated wave functions

Structure and dynamics of electronically excited molecular systems

REFERENCES

- 1. Krylov AI. The quantum chemistry of open-shell species. Rev Comp Chem. 2017;30:151-224.
- 2. Forrest SR, Thompson ME. Introduction: organic electronics and optoelectronics. Chem Rev. 2007;107:923-5.
- 3. Romero NA, Nicewicz DA. Organic Photoredox catalysis. Chem Rev. 2016;116:10075-166.
- 4. Middleton CT, de La Harpe K, Su C, Law YK, Crespo-Hernandez CE, Kohler B. DNA excited-state dynamics: from single bases to the double helix. Annu Rev Phys Chem. 2009;60:217–39.
- 5. Dreuw A, Head-Gordon M. Single-reference ab initio methods for the calculation of excited states of large molecules. Chem Rev. 2005; 105:4009–37.
- Krylov AI. Equation-of-motion coupled-cluster methods for open-Shell and electronically excited species: the Hitchhiker's guide to Fock space. Annu Rev Phys Chem. 2008;59:433–62.
- 7. Dreuw A, Wormit M. The algebraic diagrammatic construction scheme for the polarization propagator for the calculation of excited states. WIREs Comp Mol Sci. 2015;5:82–95.
- 8. Herbert JM, Zhang X, Morrison AF, Liu J. Beyond time-dependent density functional theory using only single excitations: methods for computational studies of excited states in complex systems. Acc Chem Res. 2016;49:931–41.
- 9. Lischka H, Nachtigallová D, Aquino AJA, Szalay P, Plasser F, Machado FBC, et al. Multireference approaches for excited states of molecules. Chem Rev. 2018;118:7293–361.
- 10. Jagau T-C, Bravaya KB, Krylov AI. Extending quantum chemistry of bound states to electronic resonances. Annu Rev Phys Chem. 2017; 68:525–53.
- Kimber P, Plasser F. Toward an understanding of electronic excitation energies beyond the molecular orbital picture. Phys Chem Chem Phys. 2020;22:6058–80.
- 12. Krylov AI. From orbitals to observables and back. J Chem Phys. 2020;153:080901.
- 13. Luzanov AV, Sukhorukov AA, Umanskii VE. Application of transition density matrix for analysis of excited states. Theor Exp Chem. 1976;10:354–61.
- 14. Head-Gordon M, Grana AM, Maurice D, White CA. Analysis of electronic transitions as the difference of electron attachment and detachment densities. J Chem Phys. 1995;99:14261–70.
- 15. Martin RL. Natural transition orbitals. J Chem Phys. 2003;118:4775–7.
- 16. Peach MJG, Benfield P, Helgaker T, Tozer DJ. Excitation energies in density functional theory: an evaluation and a diagnostic test. J Chem Phys. 2008;128:44118.
- Luzanov AV, Zhikol OA. Electron invariants and excited state structural analysis for electronic transitions within CIS, RPA, and TDDFT models. Int J Quantum Chem. 2010;110:902–24.
- 18. Etienne T, Assfeld X, Monari A. New insight into the topology of excited states through detachment/attachment density matrices-based centroids of charge. J Chem Theory Comput. 2014;10:3906–14.
- 19. Adamo C, Le Bahers T, Savarese M, Wilbraham L, Garcia G, Fukuda R, et al. Exploring excited states using time dependent density functional theory and density-based indexes. Coord Chem Rev. 2015;304–305:166–78.
- 20. Stein CJ, Reiher M. Measuring multi-configurational character by orbital entanglement. Mol Phys. 2017;115:2110-9.
- 21. Coleman AJ. Structure of fermion density matrices. Rev Mod Phys. 1963;35:668-86.
- 22. Davidson ER. Reduced density matrices in quantum chemistry. New York: Academic Press; 1976.
- Plasser F, Wormit M, Dreuw A. New tools for the systematic analysis and visualization of electronic excitations. I. Formalism. J Chem Phys. 2014;141:024106.
- 24. Plasser F. TheoDORE: a toolbox for a detailed and automated analysis of electronic excited state computations. J Chem Phys. 2020;152:084108.
- Plasser F, Lischka H. Analysis of Excitonic and charge transfer interactions from quantum chemical calculations. J Chem Theory Comput. 2012;8:2777–89.
- Nogueira JJ, Plasser F, González L. Electronic delocalization, charge transfer and hypochromism in the UV absorption spectrum of polyadenine unravelled by multiscale computations and quantitative wavefunction analysis. Chem Sci. 2017;8:5682–91.
- 27. Glöcklhofer F, Rosspeintner A, Pasitsuparoad P, Eder S, Fröhlich J, Angulo G, et al. Effect of symmetric and asymmetric substitution on the optoelectronic properties of 9,10-dicyanoanthracene. Mol Syst Des Eng. 2019;4:951–61.
- 28. Kimber P, Goddard P, Wright IA, Plasser F. The role of excited-state character, structural relaxation, and symmetry breaking in enabling delayed fluorescence activity in push-pull chromophores. Phys Chem Chem Phys. 2021;23:26135–50. https://doi.org/10.1039/D1CP03792G
- Mai S, Plasser F, Dorn J, Fumanal M, Daniel C, González L. Quantitative wave function analysis for excited states of transition metal complexes. Coord Chem Rev. 2018;361:74–97.

- 30. Bäppler SA, Plasser F, Wormit M, Dreuw A. Exciton analysis of many-body wave functions: bridging the gap between the quasiparticle and molecular orbital pictures. Phys Rev A. 2014;90:052521.
- 31. Plasser F, Thomitzni B, Bäppler SA, Wenzel J, Rehn DR, Wormit M, et al. Statistical analysis of electronic excitation processes: spatial location, compactness, charge transfer, and electron-hole correlation. J Comput Chem. 2015;36:1609–20.
- 32. Mewes SA, Plasser F, Dreuw A. Universal exciton size in organic polymers is determined by nonlocal orbital exchange in time-dependent density functional theory. J Phys Chem Lett. 2017;8:1205–10.
- 33. Wenzel J, Dreuw A. Physical properties, exciton analysis, and visualization of core-excited states: an intermediate state representation approach. J Chem Theory Comput. 2016;12:1314–30.
- 34. Plasser F, Bäppler SA, Wormit M, Dreuw A. New tools for the systematic analysis and visualization of electronic excitations. II. Applications. J Chem Phys. 2014;141:024107.
- 35. Gulania S, Kjønstad EF, Stanton JF, Koch H, Krylov AI. Equation-of-motion coupled-cluster method with double electron-attaching operators: theory, implementation, and benchmarks. J Chem Phys. 2021;154:114115.
- 36. Plasser F, Dreuw A. High-level ab initio computations of the absorption spectra of organic iridium complexes. J Phys Chem A. 2015;119:1023-6.
- 37. Plasser F. Entanglement entropy of electronic excitations. J Chem Phys. 2016;144:194107.
- 38. Ivanov MV, Gulania S, Krylov AI. Two cycling centers in one molecule: communication by through-bond interactions and entanglement of the unpaired electrons. J Phys Chem Lett. 2020;11:1297–304.
- 39. Plasser F, Pašalic H, Gerzabek MH, Libisch F, Reiter R, Burgdörfer J, et al. The multiradical character of one- and two-dimensional graphene nanoribbons. Angew Chem Int Ed. 2013;52:2581-4.
- 40. Orms N, Rehn DR, Dreuw A, Krylov AI. Characterizing bonding patterns in Diradicals and Triradicals by density-based wave function analysis: a uniform approach. J Chem Theory Comput. 2018;14:638–48.
- 41. Skomorowski W, Gulania S, Krylov AI. Bound and continuum-embedded states of cyanopolyyne anions. Phys Chem Chem Phys. 2018; 20:4805–17.
- 42. Plasser F. Visualisation of electronic excited-state correlation in real space. ChemPhotoChem. 2019;3:702-6.
- 43. Skomorowski W, Krylov AI. Real and imaginary excitons: making sense of resonance wave functions by using reduced state and transition density matrices. J Phys Chem Lett. 2018;9:4101–8.
- 44. Pokhilko P, Krylov AI. Quantitative El-Sayed rules for many-body wave functions from spinless transition density matrices. J Phys Chem Lett. 2019;10:4857–62.
- 45. Nanda KD, Krylov AI. Visualizing the contributions of virtual states to two-photon absorption cross sections by natural transition orbitals of response transition density matrices. J Phys Chem Lett. 2017;8:3256–65.
- 46. Nanda KD, Krylov AI. A simple molecular orbital picture of RIXS distilled from many-body damped response theory. J Chem Phys. 2020;152:244118.
- 47. Nanda KD, Krylov AI. The orbital picture of the first dipole hyperpolarizability from many-body response theory. J Chem Phys. 2021; 154:184109.
- 48. Epifanovsky E, Gilbert ATB, Feng X, Lee J, Mao Y, Mardirossian N, et al. Software for the frontiers of quantum chemistry: an overview of developments in the Q-Chem 5 package. J Chem Phys. 2021;155:084801.
- 49. Schirmer J. Beyond the random-phase approximation: a new approximation scheme for the polarization propagator. Phys Rev A. 1982; 26:2395–416.
- 50. Casanova D, Krylov AI. Spin-flip methods in quantum chemistry. Phys Chem Chem Phys. 2020;22:4326-42.
- 51. Plasser F, Mewes SA, Dreuw A, González L. Detailed wave function analysis for multireference methods: implementation in the Molcas Program package and applications to tetracene. J Chem Theory Comput. 2017;13:5343–53.
- 52. Fdez I, Galván, Vacher M, Alavi A, Angeli C, Aquilante F, et al. OpenMolcas: from source code to insight. J Chem Theory Comput. 2019;15:5925-64.
- 53. Andersson K, Malmqvist PA, Roos BO, Sadlej AJ, Wolinski K. Second-order perturbation theory with a CASSCF reference function. J Chem Phys. 1990;94:5483–8.
- 54. Klaiman S, Cederbaum LS. The best orbital and pair function for describing ionic and excited states on top of the exact ground state. J Chem Phys. 2014;141:194102.
- 55. Matsika S, Feng X, Luzanov AV, Krylov AI. What we can learn from the norms of one-particle density matrices, and what we can't: some results for interstate properties in model singlet fission systems. J Phys Chem A. 2014;118:11943–55.
- 56. Rohlfing M, Louie SG. Optical excitations in conjugated polymers. Phys Rev Lett. 1999;82:1959-62.
- 57. van der Horst JW, Bobbert PA, Michels MA, Bässler H. Calculation of excitonic properties of conjugated polymers using the Bethe–Salpeter equation. J Chem Phys. 2001;114:6950–7.
- 58. Richard RM, Herbert JM. Time-dependent density-functional description of the ¹La state in polycyclic aromatic hydrocarbons: charge-transfer character in disguise? J Chem Theory Comput. 2011;7:1296–306.
- Sánchez-Murcia PA, Nogueira JJ, Plasser F, González L. Orbital-free photophysical descriptors to predict directional excitations in metal-based photosensitizers. Chem Sci. 2020;11:7685–93.
- Clark AE, Adams H, Hernandez R, Krylov AI, Niklasson AMN, Sarupria S, et al. The middle science: traversing scale in complex manybody systems. ACS Central Sci. 2021;7:1271–87.
- 61. Tretiak S, Mukamel S. Density matrix analysis and simulation of electronic excitations in conjugated and aggregated molecules. Chem Rev. 2002;102;3171–212.
- 62. Head-Gordon M. Characterizing unpaired electrons from the one-particle density matrix. Chem Phys Lett. 2003;372:508–11.

- 63. Pletzer M, Plasser F, Rimmele M, Heeney M, Glöcklhofer F. [2.2.2.2]Paracyclophanetetraenes (PCTs): cyclic structural analogues of poly(p-phenylene vinylene)s (PPVs). Open Res Eur. 2021;1:111.
- 64. Pei Z, Ou Q, Mao Y, Yang J, Lande ADL, Plasser F, et al. Elucidating the electronic structure of a delayed fluorescence emitter via orbital interactions, excitation energy components, charge-transfer numbers, and vibrational reorganization energies. J Phys Chem Lett. 2021;12:2712–20.
- Mewes SA, Mewes J-M, Plasser F, Dreuw A. Excitons in poly(para phenylene vinylene): a quantum-chemical perspective based on highlevel ab initio calculations. Phys Chem Chem Phys. 2016;18:2548–63.
- 66. Davidson ER. The spatial extent of the V state of ethylene and its relation to dynamic correlation in the cope rearrangement. J Phys Chem. 1996;100:6161-6.
- 67. Boggio-Pasqua M, Bearpark MJ, Klene M, Robb MA. A computational strategy for geometry optimization of ionic and covalent excited states, applied to butadiene and hexatriene. J Chem Phys. 2004;120:7849–60.
- 68. Angeli C. On the nature of the $\pi \to \pi^*$ ionic excited states: the V state of ethene as a prototype. J Comput Chem. 2009;30:1319–33.
- 69. Laurent AD, Jacquemin D. TD-DFT benchmarks: a review. Int J Quantum Chem. 2013;113:2019-39.
- 70. Kozma B, Tajti A, Demoulin B, Izsák R, Nooijen M, Szalay PG. A new benchmark set for excitation energy of charge transfer states: systematic investigation of coupled cluster type methods. J Chem Theory Comput. 2020;16:4213–25.
- 71. Mewes SA, Plasser F, Dreuw A. Communication: exciton analysis in time-dependent density functional theory: how functionals shape excited-state characters. J Chem Phys. 2015;143:171101.
- 72. Mewes SA, Plasser F, Krylov A, Dreuw A. Benchmarking excited-state calculations using exciton properties. J Chem Theory Comput. 2018;14:710–25.
- 73. Grimme S, Parac M. Substantial errors from time-dependent density functional theory for the calculation of excited states of large π systems. ChemPhysChem. 2003;4:292–5.
- 74. Lee C, Yang W, Parr RG. Development of the Colle-Salvetti correlation-energy formula into a functional of the electron density. Phys Rev B. 1988;37:785–9.
- 75. Becke AD. Density-functional thermochemistry. III. The role of exact exchange. J Chem Phys. 1993;98:5648-52.
- 76. Yanai T, Tew DP, Handy NC. A new hybrid exchange–correlation functional using the coulomb-attenuating method (CAM-B3LYP). Chem Phys Lett. 2004;393:51–7.
- 77. Dreuw A, Weisman JL, Head-Gordon M. Long-range charge-transfer excited states in time-dependent density functional theory require non-local exchange. J Chem Phys. 2003;119:2943–6.
- 78. Tretiak S, Igumenshchev K, Chernyak VY. Exciton sizes of conducting polymers predicted by time-dependent density functional theory. Phys Rev B. 2005;71:33201.
- 79. Kraner S, Scholz R, Plasser F, Koerner C, Leo K. Exciton size and binding energy limitations in one-dimensional organic materials. J Chem Phys. 2015;143:244905.
- 80. Alessio M, Krylov AI. Equation-of-motion coupled-cluster protocol for calculating magnetic properties: theory and applications to single-molecule magnets. J Chem Theory Comput. 2021;17:4225–41.
- 81. Pokhilko P, Epifanovsky E, Krylov AI. General framework for calculating spin-orbit couplings using spinless one-particle density matrices: theory and application to the equation-of-motion coupled-cluster wave functions. J Chem Phys. 2019;151:034106.
- 82. El-Sayed MA. Triplet state. Its radiative and nonradiative properties. Acc Chem Res. 1968;1:8-16.
- 83. Nanda KD, Krylov AI. Two-photon absorption cross sections within equation-of-motion coupled-cluster formalism using resolution-of-the-identity and Cholesky decomposition representations: theory, implementation, and benchmarks. J Chem Phys. 2015;142:064118.
- 84. Knippenberg S, Rehn DR, Wormit M, Starcke JH, Rusakova IL, Trofimov AB, et al. Calculations of nonlinear response properties using the intermediate state representation and the algebraic-diagrammatic construction polarization propagator approach: two-photon absorption spectra. J Chem Phys. 2012;136:064107.
- 85. Kállay M, Gauss J. Calculation of frequency-dependent polarizabilities using general coupled-cluster models. J Mol Struct (THEOCHEM). 2006;768:71–7.
- 86. Plasser F, Glöcklhofer F. Visualisation of chemical shielding tensors (VIST) to elucidate aromaticity and antiaromaticity. Eur J Org Chem. 2021;2021:2529–39.
- 87. Luzanov AV, Casanova D, Feng X, Krylov AI. Quantifying charge resonance and multiexciton character in coupled chromophores by charge and spin cumulant analysis. J Chem Phys. 2015;142:224104.
- 88. Skomorowski W, Krylov AI. Feshbach–Fano approach for calculation of auger decay rates using equation-of-motion coupled-cluster wave functions. I. Theory and implementation. J Chem Phys. 2021;154:08124.
- 89. Pei Z, Yang J, Deng J, Mao Y, Wu Q, Yang Z, et al. Analysis and visualization of energy densities. II. Insights from linear-response time-dependent density functional theory calculations. Phys Chem Phys. 2020;22:26852–64.

SUPPORTING INFORMATION

Additional supporting information may be found in the online version of the article at the publisher's website.

How to cite this article: Plasser F, Krylov AI, Dreuw A. libwfa: Wavefunction analysis tools for excited and open-shell electronic states. WIREs Comput Mol Sci. 2022;e1595. https://doi.org/10.1002/wcms.1595